J. theor. Biol. (1998) **191,** 451–462

Virus Dynamics: the Effect of Target Cell Limitation and Immune Responses on Virus Evolution

ROLAND R. REGOES, DOMINIK WODARZ AND MARTIN A. NOWAK

Department of Zoology, University of Oxford, Oxford, OX1 3PS, U.K.

(*Received on* 12 *August* 1997, *Accepted in revised form on* 18 *December* 1997)

Earlier models of virus evolution during single infections do not include target cell limitation. Here we extend the basic mathematical framework of these theories and study the effect of target cell limitation on the evolution of antigenic variation, increasing replication rates and increasing virus load. We find that target cell limitation provides a selection pressure against antigenic diversification, and can therefore provide a limit to diversity. Antigenic diversity increases virus load; at the maximum level of antigenic diversity, virus load, too, is at a maximum.

1. Introduction

Mathematical models of virus infections are increasingly common. Most models have been developed for HIV-1, because this is the best studied human virus; more quantitative information is available for HIV-1 than for any other human or animal virus.

Mathematical models of HIV-1 infection have been developed to describe the continuous virus replication and evolution in the presence of immune responses (Nowak *et al*., 1990, 1991, 1995; DeBoer & Boerlijst, 1994), the interaction between HIV-1 replication and antigenic stimulation (Anderson & May, 1989; McLean & Nowak, 1992a), the consequence of anti-viral drug treatment on emergence of viral resistance (McLean & Nowak, 1992b; Frost & McLean, 1994; Stilianakis *et al*., 1997; Bonhoeffer *et al*., 1997a; Bonhoeffer & Nowak, 1997) and, more generally, the interaction between virus replication and CD4 T cells (Perelson, 1989; Perelson *et al*., 1993; DeBoer & Boucher, 1996). More recently, in conjunction with precise measurement of changes in virus load in patients receiving potent anti-viral therapy, mathematical models helped to provide estimates for rate constants of HIV-1 dynamics (Ho *et al*., 1995; Wei *et al*., 1995; Perelson *et al*., 1996, 1997; Herz *et al*., 1996; Nowak *et al*., 1995, 1997a; Bonhoeffer *et al*., 1997b) and other viruses (Nowak *et al*., 1996b, 1997b; Lifson *et al*., 1997).

In this paper, we extend earlier work (Nowak *et al*., 1991; Nowak & Bangham, 1996; Bittner *et al*., 1997) on the effect of antigenic diversity, viral replication rates and immune responses on virus load. It has been suggested that disease progression in HIV-1 infection is a consequence of virus evolution during individual infections. There are numerous experimental results suggesting (i) that HIV-1 evolves rapidly during the course of infection (Hahn *et al*., 1986; Holmes *et al*., 1992; Simmonds *et al*., 1991; Bonhoeffer *et al*., 1995; Cheynier *et al*., 1994; Meyerhans *et al*., 1989); (ii) that the virus generates mutants which escape from specific immune responses (Phillips *et al*., 1991; Nowak *et al*., 1995; Borrow *et al*., 1997; Goulder *et al*., 1997; Price *et al*., 1997); and (iii) that the virus can evolve toward faster replication rates (Asjo *et al*., 1986; Tersmette *et al*., 1989).

The evolutionary theory of HIV-1 disease progression is based on the following assumptions: (i) virus load causes disease; (ii) immune responses reduce virus load; (iii) HIV-1 can impair immune responses by killing CD4 cells; (iv) there is continuous and rapid virus replication throughout the course of infection; (v) the rapid turnover leads to a large number of virus mutants; (vi) some of these mutants

0022–5193/98/080451 + 12 $25.00/0/jt970617

can escape from immune responses; (vii) the virus may evolve towards faster replication rates during infection. Central to the evolutionary theory is the concept of an antigenic diversity threshold: if the antigenic diversity of the virus population in a patient is below a critical value then the virus population in this patient is largely controlled by specific immune responses. If the antigenic diversity exceeds this value then the immune response can no longer limit the virus population; in this case the virus will only be controlled by target cell availability.

The magnitude of the diversity threshold should vary in different people and depends (among other things) on the overall strength of the immune response of a patient. In a weak responder the diversity threshold can be low (effectively less than one strain); disease progression can occur rapidly and in the absence of significant antigenic variation. In a strong immune responder the threshold will be high, disease progression should be slow and be accompanied by the accumulation of high levels of antigenic variation. This result of the theory is not generally understood (Wolinsky *et al*., 1996; Nowak *et al*., 1996a).

More generally the diversity threshold should be interpreted as a control threshold defining whether or not the virus population is controlled (reduced) by immune responses (Nowak & May, 1992; McLean, 1993). The basic idea is that there is a dynamic balance between virus replication and immune responses which determines the level of steady-state virus load and CD4 cell counts. Any mechanism of HIV-1 disease progression has to explain how the steady state is shifted towards increasing virus load and falling CD4 cell levels (usually over the time scale of many years). The rapid turnover dynamics in itself (Ho *et al*., 1995; Wei *et al*., 1995) does not represent a mechanism of disease progression. Acording to the evolutionary theory, virus load increases slowly as a consequence of virus evolution in individual infection.

The original models of antigenic variation (Nowak *et al*., 1990) did not include target cell limitation; there the aim was to present the *simplest possible* model to study the effect of antigenic variation and evolution of virus replication rates on virus load and disease progression.

In this paper we will analyse the consequence of target cell limitation on virus load and antigenic diversity. In Section 2, we present the basic model of antigenic variation under target cell limitation without immune function impairment. Therefore, the basic model applies to a virus which does not impair the immune system. In Sections 3 and 4, we extend this model by including different mathematical expressions of immune function impairment (which is a specific feature of HIV-1 infection.) Finally, in Section 5 we analyse the consequences of immune function impairment in a model with a different mathematical term of immune response activation.

2. Model without Immune Function Impairment

At first we consider a model that describes the interaction between susceptible cells, x, different strains of virus particles, v_i, infected cells, y_i, and strain specific immune responses, z_i. There are n different strains of virus, therefore $i = 1, \ldots, n$. We assume that susceptible cells, x are produced at a constant rate, λ, and die at rate dx. Infection by virus of type i turns them into infected cells, y_i, at a rate $\beta_i' x v_i$. Infected cells, y_i, die at rate ay_i and are killed by the strain specific immune responses at rate py_iz_i. The strain specific immune responses, z_i, are stimulated at a rate cy_iz_i and decline at rate bz_i. Virus particles, v_i, are produced by infected cells at rate κy_i and are cleared at rate uv_i. These assumptions lead to the following system of differential equations:

$$\mathrm{d}x/\mathrm{d}t = \lambda - \mathrm{d}x - \sum_{i=1}^{n} \beta_i' x v_i \tag{1}$$

$$\mathrm{d}y_i/\mathrm{d}t = \beta_i' x v_i - a y_i - p y_i z_i \tag{2}$$

$$\mathrm{d}z_i/\mathrm{d}t = c y_i z_i - b z_i \tag{3}$$

$$\mathrm{d}v_i/\mathrm{d}t = \kappa y_i - u v_i \tag{4}$$

Note that due to the special form of the immune response term $cy_iz_i - bz_i$, this model requires infected cell load to exceed a threshold level, $y_i = b/c$, for immune stimulation to occur. We call this level *stimulation threshold*.

If the decay rate of free virus, u, is much larger than the decay rate of the virus producing infected cell population, a, then we may assume to a good approximation that virus is in steady state (i.e. $\mathrm{d}v_i/\mathrm{d}t = 0$) and thus $v_i = (\kappa/u)y_i$. This leads to the simplified system of differential equations:

$$\mathrm{d}x/\mathrm{d}t = \lambda - \mathrm{d}x - \sum_{i=1}^{n} \beta_i x y_i \tag{5}$$

$$\mathrm{d}y_i/\mathrm{d}t = \beta_i x y_i - a y_i - p y_i z_i \tag{6}$$

$$\mathrm{d}z_i/\mathrm{d}t = c y_i z_i - b z_i \tag{7}$$

where $\beta_i = (\kappa/u)\beta_i'$. Without loss of generality we label the strains such that $\beta_1 > \beta_2 > \ldots > \beta_n$.

2.1. EQUILIBRIUM SOLUTIONS

The number of virus strains which coexist at equilibrium or the *antigenic diversity* of the system is given by the largest index m, such that $\beta_m\xi_{m-1} > a$, where $\xi_{m-1} := \lambda/[d + (b/c)\ \Sigma_{j=1}^{m-1}\ \beta_j]$. If, in addition $\beta_m\xi_m > a$, then strain m induces an immune response, z_m at equilibrium.

There is only one globally stable equilibrium because β_i and ξ_i are monotonously decreasing for increasing index i. Thus $\beta_1\xi_0$, $\beta_1\xi_1$. $\beta_2\xi_1$. $\beta_2\xi_2$, . . ., $\beta_n\xi_{n-1}$, $\beta_n\xi_n$ is a decreasing series of real numbers. After having determined the diversity, m, as above, the only possibilities left are $\beta_m\xi_m > a$ or $\beta_m\xi_m < a$, corresponding to non-vanishing and vanishing immune response, z_m, respectively.

Thus there are two types of possible equilibrium solutions to this system.

(1) The first type of equilibrium contains m strains of infected cells, $y_i > 0$, for $i = 1, \ldots, m$, which are controlled by m strain specific immune responses, $z_i > 0$, $i = 1, \ldots, m$. The equilibrium levels are:

$$\hat{x} = \lambda/[d + (b/c)\sum_{j=1}^{m}\beta_j] \tag{8}$$

$$\hat{y}_i = \begin{cases} b/c & i = 1, \ldots, m \\ 0 & i = m+1, \ldots, n \end{cases} \tag{9}$$

$$\hat{z}_i = \begin{cases} (\beta_i\hat{x} - a)/p & i = 1, \ldots, m \\ 0 & i = m+1, \ldots, n \end{cases} \tag{10}$$

(2) In the second type of equilibrium, m virus strains are opposed by only $m - 1$ immune responses. The m-th strain is controlled by target cell availability. The equilibrium levels are:

$$\hat{x} = a/\beta_m \tag{11}$$

$$\hat{y}_i = \begin{cases} b/c & i = 1, \ldots, m-1 \\ \lambda/a - \lambda/(\beta_m\xi_{m-1}) & i = m \\ 0 & i = m+1, \ldots, n \end{cases} \tag{12}$$

$$\hat{z}_i = \begin{cases} (\beta_i/\beta_m - 1)a/p & i = 1, \ldots, m-1 \\ 0 & i = m, \ldots, n \end{cases} \tag{13}$$

2.2. SIMULATIONS

We performed computer simulations of an infection that start with a single virus strain, and over time new virus strains i emerge with randomly distributed replication rates, β_i. In each round of the simulation a new virus strain is added to the system and the new equilibrium is calculated according to the above algorithm. Whenever a new strain is added, the system may evolve in one of the following ways:

(i) the new strain may be unable to invade the system due to a low replication rate;

(ii) the new strain may invade and drive one or several other virus strains to extinction;

(iii) the new strain may invade without eliminating other virus strains [similar models have been explored by Law & Morton (1993) and Nee & May (1992) in ecological contexts]

We obtain the following dynamics:

- an initial linear increase of the antigenic diversity, m, followed by saturation (see Fig. 1);
- an initial increase of the total abundance of infected cells, $y = \Sigma_{i=1}^{m}\ \hat{y}_i$, followed by constancy;
- an increase of the total immune response, $z = \Sigma_{i=1}^{m}\ \hat{z}_i$, followed by a decline (see Fig. 2);
- a monotonous decrease of uninfected cells, x;
- a monotonous increase in the average replication rate, $\overline{\beta} = \Sigma_{i=1}^{n}\ \beta_i\hat{y}_i/y$ (see Fig. 3).

From these dynamics we are able to derive the following correclations:

- a linear correlation between the total abundance of infected cells, y, and the antigenic diversity, m (see Fig. 4);

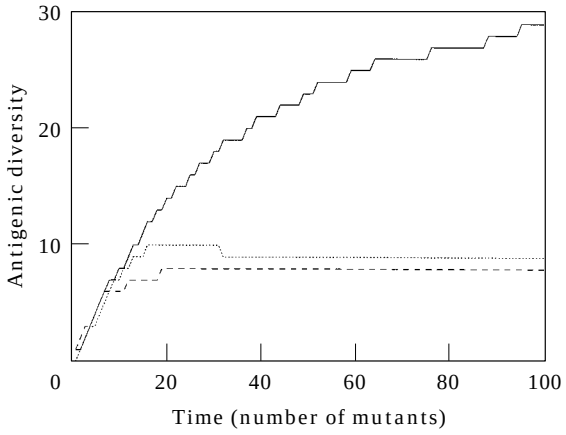

FIG. 1. Evolution of virus diversity in the course of infection for the model without impairment of Section 2 (solid line), for the model with direct impairment of Section 3 (dashed line) and the model with indirect impairment of Section 4.2 (dotted line); the x-axis (time) indicates the number of mutants which have been generated since the beginning of infection; the y-axis (antigenic diversity) represents the actual number of mutants present in the system; the saturated level of diversity in the cases with impairment is markedly lower than in the case without impairment; in our simulations we used the following parameters: $\lambda = 1.0$, $d = 0.01$, $a = 0.5$, $p = 1.0$, $c = 1.0$, $b = 0.05$ and $\mu = 0.1$ and uniformly distributed replication rates, $\beta \in [0, 0.05]$; to be able to compare the cases with direct and indirect impairment we adjusted ζ such that we obtain similar diversity suppression.

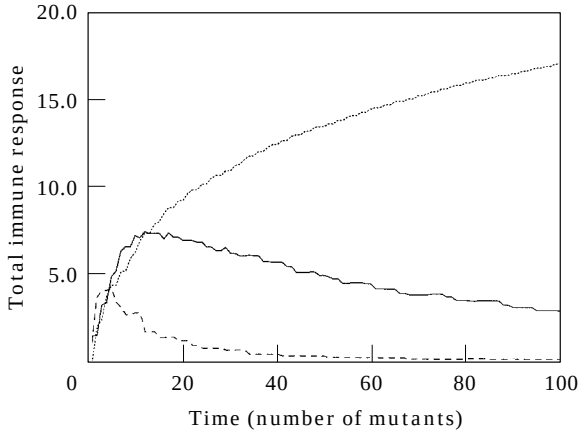

FIG. 2. Progressions of immune cell load for the model of Section 2 (solid curve), the model of Section 3 (dashed curve) and the model of Section 5 without impairment (dotted curve); the introduction of impairment into the model of Section 2 results in immune cell exhaustion; the model of Section 5 with the stimulation term cy_i, on the other hand, displays a monotonous increase of immune cell load in the course of infection.

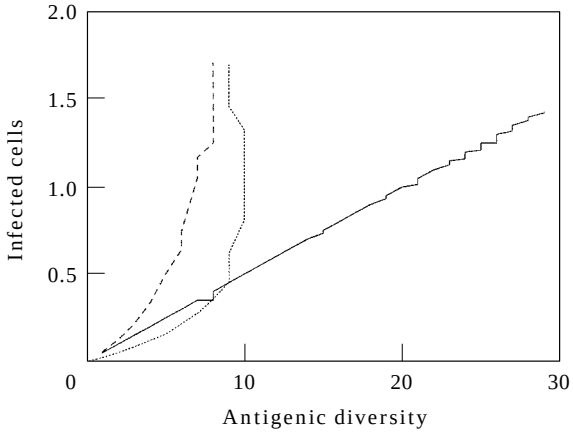

FIG. 4. Correlation between the equilibrium abundance of infected cells and antigenic diversity; solid, dashed and dotted curves represent the cases without, with direct and with indirect impairment, respectively; introduction of impairment of immune function changes the linear correlation between the infected cell load and the diversity to convex correlations.

• a positive, approximately linear correlation between the average replication rate, β, and the antigenic diversity, m.

2.3. INTERPRETATION OF RESULTS

To interpret the results presented in the previous subsection it is appropriate to focus on the effects and the balance of the different selection pressures that act on the virus population. On the one hand, there is the pressure exerted by the immune responses on virus population that controls virus growth. Virus abundance can, nevertheless, be high if the number of virus strains is sufficiently large. An increase of antigenic diversity can thus be viewed as an escape of the virus population from immune selection pressure. On the other hand, the limitation in target cells introduces competition among different virus strains, and therefore acts against the establishment of high antigenic diversity in the virus population. The progressions and correlations that were presented in the preceding subsection, are the result of the balance between these two forces.

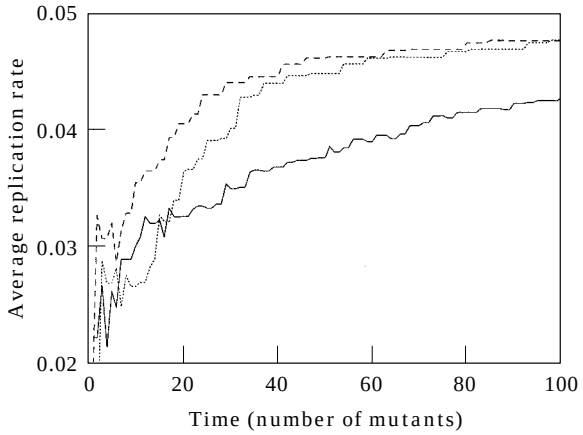

FIG. 3. Progression of the average replication rate $\overline{\beta} = \Sigma_{i=1}^{n} \beta_i y_i / y$, in the models of Sections 2, 3 and 4.2 (solid, dashed and dotted curves, respectively); impairment results in a higher final level of the average replication rate; in the model of Section 3 this higher level is attained faster than in the model of Section 4.2.

The linear increase of the antigenic diversity in the beginning of the infection can be interpreted as an escape of the virus population from the selection pressure exerted by the immune responses. In the later stages of the infection, however, the target cell limitation becomes more influential and leads to the saturation of antigenic diversity (cf. Fig. 1). There is a maximum number of virus strains that can coexist at equilibrium. This represents a limit of antigenic diversity.

Since the number of target cells is limited, the abundance of infected cells and thus virus load (which is proportional to the number of infected cells in our models) cannot grow indefinitely in the course of infection, but has to terminate at some maximum level. This level is attained by the establishment of virus strains, each with the abundance $v_i = \kappa b/(uc)$. The contribution of each strain to the total virus load is independent of the antigenic diversity, m, which is the reason for the linearity of the correlation between the total abundance of infected cells and the antigenic diversity (cf. Fig. 4).

The equilibrium virus load, which is achieved for the maximum antigenic diversity, is equivalent to the carrying capacity of the system. The carrying capacity is defined as the equilibrium virus load that would be

achieved by a virus strain with maximum replication rate in the absence of immune response.

As a result of the competition between the different virus strains in target cell limited systems, the average replication rate, β, increases in the course of infection.

2.4. APPROXIMATIONS FOR UNIFORM DISTRIBUTION OF REPLICATION RATES

For a large number of mutants, n, one can derive diversity-dependent expressions for the equilibrium values of the susceptible cell population, x, of the total abundance of infected cells, y, and the total frequency of immune cells, z:

$$x_{appr} = \frac{\lambda}{d + (b/c)\sigma} \tag{14}$$

$$y_{appr} = \frac{mb}{c} \tag{15}$$

$$z_{appr} = \frac{\lambda\sigma}{p(d + (b/c)\sigma} - \frac{ma}{p} \tag{16}$$

where $\sigma = Bm[1 - (m/2n)]$. Here we have assumed a uniform distribution of infection rates, β_i, in an interval $[0,\beta]$, which leads to $\beta_i \approx B[1 - (i/n)]$ and $\Sigma_{j=0}^{m} \beta_j \approx Bm[1 - (m/2n)] = \sigma$, and we have approximated $m - 1 \approx m$. Note that the diversity, m, depends on n.

These expressions can be simplified by considering two limiting cases of the correlation between the antigenic diversity, m, and the total number of strains, n, generated in the course of infection. In our simulations the number n plays also the role of a discrete time variable—the ticking of a clock with variable speed, counting the emergence of new mutants. In the beginning of simulations one can observe a linear increase of the antigenic diversity, m. Thus, initially, we have $(m/n) \approx 1$. In the end of our simulations, i.e. for large n, the diversity m is almost constant. We therefore have $(m/n) \approx 0$. This latter approximation is equivalent to the limit of equal replication rates, $\beta_i = B$, $i = 1, \ldots, n$.

These two further approximations lead to the following, very similar expressions, which provide boundaries for the exact correlations (see Fig. 5):

$$x_{appr1}(m) = \lambda[d + (b/c)B(m/2)] \tag{17}$$

$$x_{appr2}(m) = \lambda[d + (b/c)Bm] \tag{18}$$

$$z_{appr1}(m) = \lambda Bm/[p(2d + (b/c)Bm)] - ma/p \tag{19}$$

$$z_{appr2}(m) = \lambda Bm/[p(d + b/c)Bm)] - ma/p \tag{20}$$

By considering the approximate condition of invasion for the m-th strain, $\beta_m x_{appr2} > a$, we get an expression for the saturated level of diversity, m_{sat}, in this model:

$$m_{sat} = \lambda c/(ab) - cd/(bB) \tag{21}$$

which is approximately

$$m_{sat} \approx \lambda c/(ab) \tag{22}$$

for large replication rates (cf. Fig. 1).

3. Model with Immune Function Impairment

Let us now consider the above model extended by an immune response impairment term, $-\mu y_i$, where $y = \Sigma_{i=1}^{n} y_i$:

$$dx/dt = \lambda - dx - \sum_{i=1}^{n} \beta_i x y_i \tag{23}$$

$$dy_i/dt = \beta_i x y_i - a y_i - p y_i z_i \tag{24}$$

$$dz_i/dt = c y_i z_i - b z_i - \mu y z_i \tag{25}$$

Here again $i = 1, \ldots, n$ and the βs are labeled such that $\beta_1 > \beta_2 > \ldots > \beta_n$.

This impairment term stems from a term $-\mu' v z_i$ ($v := \Sigma_{i=1}^{n} v_i$) that captures the idea of a virus-induced inhibition of strain specific immune responses, z_i. The term $-\mu' v z_i$ turns into $-\mu y z_i$ after the steady state assumption for virus particles, v_i, as above. One should note that the impairment is cross-reactive, i.e. virus strains do not distinguish between different strain specific immune cells. This extension renders the model applicable to HIV-1 infection and other virus infections with immune function impairment, as e.g. LCMV infection.

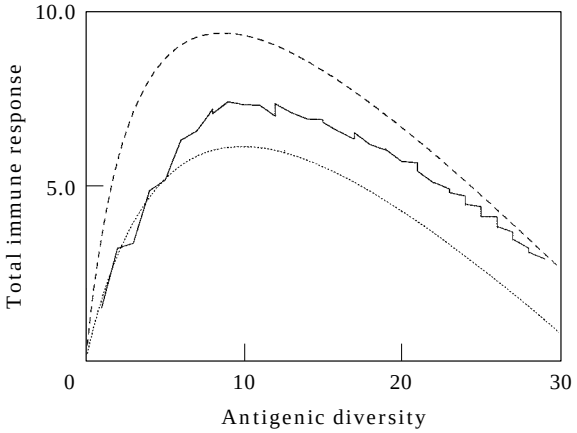

FIG. 5. Correlations between the immune cell load and the diversity for the models without impairment of Section 2; the correlations are compared with the approximate expressions eqns (19) and (20).

3.1. EQUILIBRIUM SOLUTIONS

The search for stable equilibrium solutions can be carried through analogously to the last section, since the frequency of susceptible cells in the presence of the first i strains, ξ_i, turns out to be monotonously decreasing again. We can thus define the diversity, m, to be the greatest integer fulfilling $\beta_m \xi_{m-1} > a$ where the frequency of susceptible cells in the presence of the first $(m-1)$ strains is defined as $\xi_{m-1} := \lambda / \{d + [b/(c-(m-1)\mu]\Sigma_{j=1}^{m-1} \beta_j\}$. If, additionally, $\beta_m \xi_m > a$, then the m-th immune response is induced.

The stable equilibrium solutions can again be divided into two types:

(1) The first type of equilibrium contains m strains of infected cells, $y_i > 0$, for $i = 1, \ldots, m$, which are contolled by m strain specific immune responses, $z_i > 0$, $i = 1, \ldots, m$. The equilibrium levels are:

$$\hat{x} = \lambda / \left\{ d + [b/(c - m\mu)] \sum_{j=1}^{m} \beta_j \right\} = \xi_m \tag{26}$$

$$\hat{y}_i = \begin{cases} b/(c - m\mu) & i = 1, \ldots, m \\ 0 & i = m+1, \ldots, n \end{cases} \tag{27}$$

$$\hat{z}_i = \begin{cases} (\beta_i \hat{x} - a)/p & i = 1, \ldots, m \\ 0 & i = m+1, \ldots, n \end{cases} \tag{28}$$

(2) In the second type of equilibrium, m virus strains are opposed by only $m-1$ immune responses. The m-th strain is controlled by target cell availability. The equilibrium levels are:

$$\hat{x} = a/\beta_m \tag{29}$$

$$\hat{y}_i = \begin{cases} (b + \mu\hat{y})/\mathrm{c} & i = 1, \ldots, m-1 \\ \hat{y} - (\mathrm{m}-1)(\mathrm{b} + \mu\hat{y})/c & i = m \\ 0 & i = m+1, \ldots, n \end{cases} \tag{30}$$

$$\hat{z}_i = \begin{cases} (\beta_i \hat{x} - a)/p & i = 1, \ldots, m-1 \\ 0 & i = m, \ldots, n \end{cases} \tag{31}$$

where

$$\hat{y} := \sum_{i=1}^{m} \hat{y}_i = \frac{\lambda/a - d/\beta_m)c + (m-1)b - b \sum_{j=0}^{m-1} \beta_j/\beta_m}{\mu \sum_{j=0}^{m-1} \beta_j/\beta_m + c - (m-1)\mu} \tag{32}$$

3.2. SIMULATIONS

Based on the above algorithm and the equilibrium levels, the same kind of computer simulations of an infection were performed as described in the previous section. We obtain the following dynamics:

- an initial linear increase of the diversity, m, followed by saturation (see Fig. 1); the saturated level is much lower than in the case without impairment, $\mu = 0$;
- an initial increase of the total abundance of infected cells, $y = \Sigma_{i=1}^{m} \hat{y}_i$, followed by constancy; the constant level is reached much faster than in the case without impairment;
- an increase of the total immune response, $z = \Sigma_{i=1}^{m} \hat{z}_i$ over time followed by a decline; the final level of total immune response is much lower than in the model without impairment, $\mu = 0$ (see Fig. 2); thus a model with impairment can account for the phenomenon of immune cell exhaustion, i.e. a complete loss of specific immune cells (cf. Wodarz *et al.*, 1997);
- a monotonous decrease of uninfected cells, x;
- a monotonous increase in the average replication rate, $\overline{\beta} = \Sigma_{i=1}^{n} \beta_i \hat{y}_i / y$, over time (see Fig. 3); the increase is much faster and reaches a higher level than without in the model impairment, $\mu = 0$.

From these observations we derive the following correlations:

- a positive, convex correlation between the total abundance of infected cells, y, and the diversity, m, i.e. increase is not constant as in the case without impairment, $\mu = 0$, but becomes steeper with increasing diversity, m (see Fig. 4);
- a positive, convex correlation between the average repliction rate, $\overline{\beta}$, and the antigenic diversity, m.

3.3. INTERPRETATION OF RESULTS

Since immune function impairment weakens the immune response, the virus population is more dominated by target cell limitation. As before we find that antigenic diversity, m, increases over time to a certain maximum value, but the maximum value is lower than for the case $\mu = 0$. Virus load, y, increases with increasing antigenic diversity, m. Interestingly, the slope of y vs. m increases, therefore as antigenic diversity comes closer to its maximum value each new strain has a greater effect on increasing the overall virus population size. At the maximum value of m, the virus population size is equivalent to the total carrying capacity of the system. For increasing

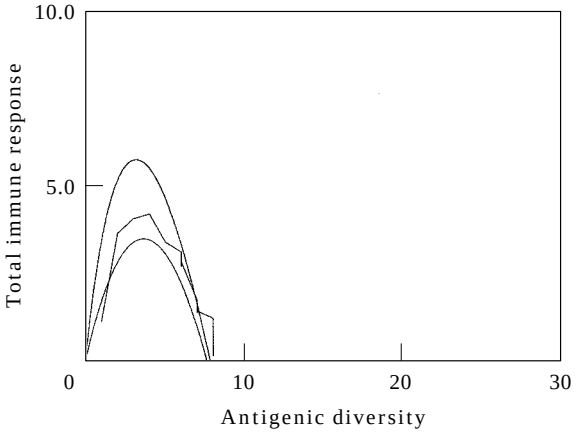

FIG. 6. Correlations between the immune cell load and the diversity for the models with impairment of Section 3; the correlations are compared with the approximate expressions eqns (36) and (37).

immune function impairment this happens at lower values of m.

3.4. APPROXIMATIONS FOR UNIFORM DISTRIBUTION OF REPLICATION RATES

By assuming a large number of strains, n, and uniformly distributed βs as in the previous section, we can derive approximate expressions for the equilibrium values of the susceptible cell population, x, of the total abundance of infected cells, y, and the total frequency of immune cells, z:

$$x^1_{appr}(m) = 2\lambda(c - m\mu)/[2d(c - m\mu) + bBm] \quad (33)$$

$$x^2_{appr}(m) = \lambda(c - m\mu)/[d(c - m\mu) + bBm] \quad (34)$$

$$y_{appr}(m) = mb/(c - m\mu) \quad (35)$$

$$z^1_{appr}(m) = 2\lambda B(c - m\mu)m/[p(2d(c - m\mu) + bBm)] - ma/p \quad (36)$$

$$z^2_{appr}(m) = \lambda B(c - m\mu)m/[p(d(c - m\mu) + bBm)] - ma/p \quad (37)$$

We find that $x^1_{appr}(m)$ is an upper estimate for the exact equilibrium value of x for a given diversity, m. Similarly $x^2_{appr}(m)$ is a lower estimate for the equilibrium number of target cells, x, for given m. In addition we have that $z^1_{appr}(m)$ is a lower estimate for the exact value of z for a given diversity, m, and $z^2_{appr}(m)$ is an upper estimate for the equilibrium abundance of the total immune response for a given m.

By considering the approximate condition of invasion for the m-th strain, $\beta_m x_{appr2} > a$, we get an expression for the saturated level of diversity, m_{sat}, in the impaired model:

$$m_{sat} = (adc - \lambda cB)/(ad\mu - \lambda\mu B - abB) \quad (38)$$

which is approximately

$$m_{sat} \approx c/(\mu + ab/\lambda) \quad (39)$$

for large replication rates (cf. Fig. 1). For $\mu \ll ab/\lambda$, this expression is equivalent to the expression for m_{sat} without impairment [eqn (22)]. For $\mu \gg ab/\lambda$, we obtain $m_{sat} \approx c/\mu$.

4. Models with Other Impairment Mechanisms

In this section we will investigate the effect of other immune function impairment mechanisms.

4.1. INFECTED-CELL-DEPENDENT IMMUNE STIMULATION RATE

At first, let us consider the case in which immune function is impaired by a reduction of the immune stimulation rate, c, induced by uninfected cells. We therefore replace c in the model of Section 2 by $c/(1 + u'y)$. The resulting model is

$$dx/dt = \lambda - dx - \sum_{i=1}^{n} \beta_i x y_i \quad (40)$$

$$dy_i/dt = \beta_i x y_i - a y_i - p y_i z_i \quad (41)$$

$$dz_i/dt = (c y_i z_i)/(1 + u'y) - b z_i \quad (42)$$

The equilibrium solutions are equivalent to the model introduced in Section 3 with an impairment term $-u y_i z_i$, where $u := u'b$. Thus the assumption of reduction of the stimulation rate, c, turns out to be equivalent to that of inhibition of immune cell growth in these models.

4.2. TARGET-CELL-DEPENDENT IMMUNE STIMULATION RATE

Another possible way to introduce cross-reactive immune function impairment is replacing $c y_i z_i$ by $\zeta x y_i z_i$. Here we identify the variable x as uninfected CD4 cells and z_i as specific CD8 cells. The activation of CD8 cells is proportional to the signals stemming from both infected cells (displayed antigen on surface) and uninfected CD4 cells (cytokine release). The model equations are:

$$dx/dt = \lambda - dx - \sum_{i=1}^{n} \beta_i x y_i \quad (43)$$

$$dy_i/dt = \beta_i x y_i - a y_i - p y_i z_i \quad (44)$$

$$dz_i/dt = \zeta x y_i z_i - b z_i \quad (45)$$

By following the same line of argument as in the previous sections, we obtain two types of equilibrium solutions:

(1) The first type of equilibrium contains m strains of infected cells, $y_i > 0$, for $i = 1, \ldots, m$, which are controlled by m strain specific immune responses, $z_i > 0$, $i = 1, \ldots, m$. The equilibrium levels are:

$$\hat{x} = \lambda/d - b \sum_{j=1}^{m} \beta_j/(\zeta d) \tag{46}$$

$$\hat{y}_i = \begin{cases} bd/[\lambda\zeta - b\Sigma_{j=1}^{m} \beta_j], & i = 1, \ldots, m \\ 0, & i = m+1, \ldots, n \end{cases} \tag{47}$$

$$\hat{z}_i = \begin{cases} (\beta_i \hat{x} - a)/p, & i = 1, \ldots, m \\ 0, & i = m+1, \ldots, n \end{cases} \tag{48}$$

(2) In the second type of equilibrium, m virus strains are compensated by only $m-1$ immune responses. The m-th strain is essentially controlled by target cell availability. The equilibrium levels are:

$$\hat{x} = a/\beta_m \tag{49}$$

$$\hat{y}_i = \begin{cases} (b\beta_m)/(a\zeta), & i = 1, \ldots, m-1 \\ \zeta_{m-1}\, d/a - d/\beta_m & i = m \\ 0 & i = m+1, \ldots, n \end{cases} \tag{50}$$

$$\hat{z}_i = \begin{cases} (\beta_i \hat{x} - a)/p, & i = 1, \ldots, m-1 \\ 0, & i = m, \ldots, n \end{cases} \tag{51}$$

where $\xi_i = \lambda/d - b\Sigma_{j=1}^{i} \beta_j/(\zeta d)$ for this model.

If we plot ξ_i as a function of i for different n, two shapes can be observed: (i) for low n, ξ_i is a decreasing function of i but always remains positive; (ii) for high n, ξ_i can become zero. The transition between these two cases plays an important role for the progression of antigenic diversity, as is explained later. The critical value of the total number of mutants n that divides the two cases can be calculated by evaluating $\xi_{n_e} = 0$, which leads to:

$$n_c = \lambda c/(b\overline{\beta}) \tag{52}$$

The same sort of simulations as in the previous sections give unexpected results: the diversity, m, of this system increases to a maximum, m_{max}, attained at n_c, but declines again to reach a saturated level m_{sat} (see Fig. 1). Thus, unlike in the models of the previous section, in the present model antigenic diversity does not increase monotonously as a function of n.

The decline of the antigenic diversity coincides with a strong increase in the average replication rate, $\overline{\beta} = \Sigma_{i=1}^{n} \beta_i y_i/y$ (see Fig. 3).

As in the model with direct immune function impairment of Section 3, we obtain a positive, convex correlation between infected cell load and antigenic diversity (see Fig. 4), which is again due to the diversity-dependence of the contributions of a virus strain to the total virus load [cf. eqn (47)].

For uniformly distributed replication rates we can approximate the saturated level of diversity by:

$$m_{sat} \approx \lambda c/(bB) - acd/(bB^2) \tag{53}$$

5. Does Target Cell Limitation Always Lead to a Limit for Antigenic Diversity?

No—as a counterexample we consider a model with a linear immune stimulation term, cy_i. Here the uninfected cell frequency does not have to exceed a threshold in order to stimulate an immune response. We have:

$$\mathrm{d}x/\mathrm{d}t = \lambda - \mathrm{d}x - \sum_{i=1}^{n} \beta_i x y_i \tag{54}$$

$$\mathrm{d}y_i/\mathrm{d}t = \beta_i x y_i - a y_i - p y_i z_i \tag{55}$$

$$\mathrm{d}z_i/\mathrm{d}t = c y_i - b z_i - \mu y z_i \tag{56}$$

5.1. EQUILIBRIUM SOLUTIONS

This system has exactly one stable equilibrium solution characterized by the diversity m:

$$\hat{x} = \lambda/(d + \eta) \tag{57}$$

$$\hat{y}_i = \begin{cases} (\beta_i \hat{x} - a)(b + \mu y)/(pc) & i = 1, \ldots, m \\ 0 & i = m+1, \ldots, n \end{cases} \tag{58}$$

$$\hat{z}_i = \begin{cases} c y_i/(b + \mu y) & i = 1, \ldots, m \\ 0 & i = m+1, \ldots, n \end{cases} \tag{59}$$

where $y = \Sigma_{i=1}^{n} y_i$ and $\eta = \Sigma_{i=1}^{n} \beta_i y_i$. The diversiry, m, is defined as the largest number fulfilling the equation of invasion $\beta_i \xi_{i-1} > a$. Here $\xi_i = \lambda/(d + \Sigma_{j=1}^{i} \beta_j y_j)$.

By summation of eqn (58) and by summation of eqn (58) multiplied by β_i, we obtain two equations for y and η, which can be easily solved. The total number of infected cells, y, in terms of η is:

$$y = \frac{\lambda b \, \Sigma_{i=1}^{m} \beta_i - mab(d + \eta)}{(ma\mu + pc)(d + \eta) - \lambda\mu \, \Sigma_{i=1}^{m} \beta_i} \tag{60}$$

The reduced infected cell load, η, is given by a polynomial of third order:

$$\gamma_3\eta^3 + \gamma_2\eta^2 + \gamma_1\eta + \gamma_0 = 0 \qquad (61)$$

with

$$\gamma_3 = (cp)^2 + macp\mu$$

$$\gamma_2 = 2d(cp)^2 + 2macdp\mu - 2ma^2b\mu \sum_{i=0}^{m}$$

$$\beta_i - cp\lambda\mu \sum_{i=0}^{m} \beta_i - abcp \sum_{i=0}^{m} \beta_i\gamma_1 = (cdp)^2$$

$$+ macd^2p\mu - 4ma^2bd\mu \sum_{i=0}^{m}$$

$$\beta_i - cdp\lambda\mu \sum_{m}^{} i = 0\ \beta_i - 2abcdp \sum_{i=0}^{m}$$

$$\beta_i - bcp\lambda \sum_{i=0}^{m} \beta_i^2 + 2ab\lambda\mu \left(\sum_{i=0}^{m} \beta_i \right)^2$$

$$\gamma_0 = -2ma^2bd^2\mu \sum_{i=0}^{m} \beta_i - abcd^2p \sum_{i=0}^{m} \beta_i$$

$$- bcdp\lambda \sum_{i=0}^{m} \beta_i^2 + 2abd\lambda\mu \left(\sum_{i=0}^{m} \beta_i \right)^2$$

In the case of no immune function impairement, $\mu = 0$, the polynomial for η is only quadratic:

$$c\eta^2 + (cd + abp \sum_{i=0}^{m} \beta_i)\eta + abdp \sum_{i=0}^{m} \beta_i$$

$$- bp\lambda \sum_{i=0}^{m} \beta_i^2 = 0 \qquad (62)$$

5.2. SIMULATION

In simulations where a new strain is added to the system every round, we obtain the following dynamics:

- an increase of antigenic diversity, m, over time without upper limit [see Fig. 7(a)]; the slope of the curve is larger for the case without impairment, $\mu = 0$;
- an initial increase of the total abundance of infected cells, $y = \Sigma[m/i = 1]\ \hat{y}_i$, followed by constancy; higher immune function impairment (larger u) results in a higher maximum level of infected cells;
- the total immune response, $z = \Sigma_{i=1}^{m}\ \hat{z}_i$, is proportional to the total abundance of infected cells, y (see Fig. 2); the total immune response does not decline, i.e. there is no immune cell exhaustion due to

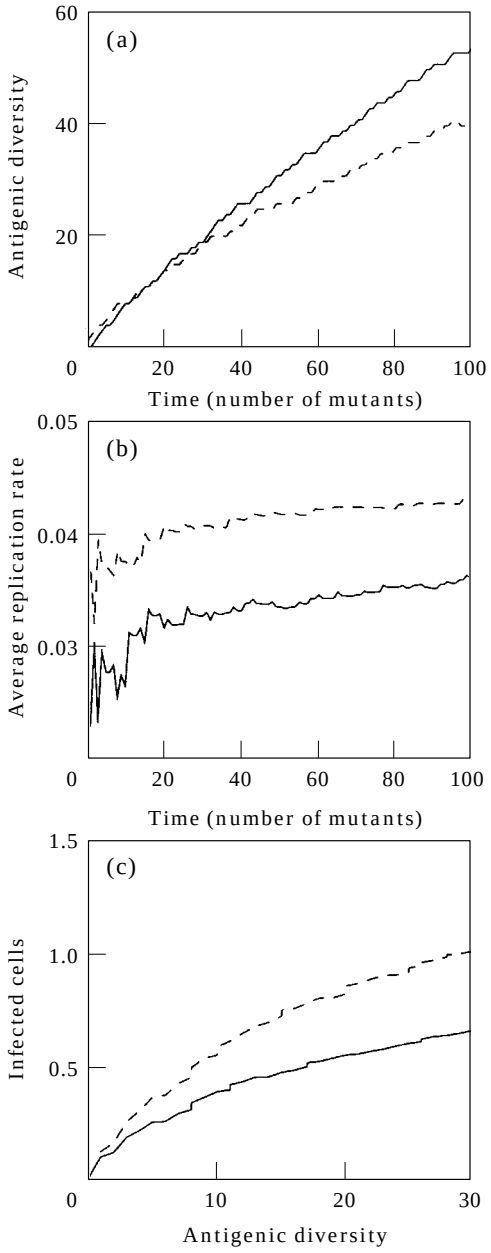

FIG. 7. (a) Evolution of virus diversity in the course of infection for the models of Section 5 with impairment (solid line) and without impairment (dashed line); though the introduction of impairment reduces the slope of the curve corresponding to the case without impairment, in either case the diversity does not saturate; (b) progression of the average replication rate $\overline{\beta} = \Sigma_{i=1}^{m}\ \beta_i y_i/y$, in the model of Section 5 without and with impairment (solid and dashed curves, respectively); again the model with impairment attains a higher final level of the average replication rate; (c) the correlations between the equilibrium abundance of infected cells and antigenic diversity for the models of Section 5; the cases without and with impairment are represented by solid and by dashed curves, respectively; immune function impairment increases virus load.

reduced target cell availability as in the previous models;

- a monotonous decrease of uninfected cells, x;
- a montonous increase of the average replication rate, $\overline{\beta} = \Sigma_{i=1}^{n} \beta_i \hat{y}_i / y$ [see Fig. 7(b)]; higher immune function impairment (larger μ) leads to an higher average replication rate, $\overline{\beta}$.

From these dynamics we derive the following correlations:

- a positive, concave correlation between the total abundance of infected cells, y, and the antigenic diversity, m, i.e. the slope of the correlation is decreasing [see Fig. 7(c)]; the stronger the immune function impairment, μ, the higher the equilibrium level of infected cells for a given antigenic diversity, m;
- a positive, concave correlation between diversity, m, and replication rate, $\overline{\beta}$.

5.3. INTERPRETATION OF RESULTS

In the model given by eqns (54)–(56) there is no immune stimulation threshold, i.e. there is no minimum number of infected cells required in order to stimulate a specific immune response. Therefore, there is no limit for the number of strains that can coexist at equilibrium. We find that antigenic diversity, m, increases over time (as given by the total number of mutants, n, generated during the course of infection). But the rate of increase of m vs. n slows down.

Virus load (in terms of infected cell numbers) increases with increasing antigenic diversity, m. For high values of m, the virus load converges to the total carrying capacity of the system. Immune function impairment always leads to higher virus load for the same value of m. As in the previous models, the average replication rate of the virus population increases during infection. The model does not show immune cell exhaustion.

6. Conclusion

In this paper, we have explored the effects of target cell limitation and immune responses on virus dynamics by analysing several mathematical models of virus infections. Starting from the basic model without immune function impairment in Section 2, we proceeded to models with impairment in Section 3 and 4. In Section 5 we investigated a model with a different mathematical term describing immune response activation dynamics.

If the number of target cells in a system is limited then virus load cannot grow indefinitely but has to terminate at some maximum level. Furthermore, target cell limitation introduces competition among virus strains and therefore acts to reduce viral diversity. Therefore, in our models there are two opposing selection pressures acting on the virus population: specific immune responses select for escape variants and thus increase antigenic diversity; target cell limitation reduces viral diversity.

We performed computer simulation of infection dynamics assuming that new antigenic variants are continuously produced during the course of infection. In the models of Sections 2, 3 and 4, where the mathematical term for the immune response stimulation is given by cy_iz_i, we observe a limit to diversity. There is a maximum number of viral strains which can coexist at equilibrium. During the course of infection the number of viral strains increases until this maximum is reached.

In our computer simulations, virus load increases with increasing antigenic diversity during the course of an infection. At the maximum level of antigenic diversity, virus load, too, is at a maximum. At this point the virus load is equivalent to the total carrying capacity of the system, which is defined as the equilibrium abundance of a visus strain with maximum replication rate in the absence of an immune response. Thus antigenic diversification eliminates the effect of the immune response and renders the virus population only subject to control by target cell availability.

Immune function impairment has the following effect in our model: for equivalent levels of antigenic diversity, virus load is higher in the case of immune function impairment. There is also a lower limit to diversity in the presence of immune function impairment. (This in intuitively obvious, because a weaker immune system provides a lower selection pressure to maintain antigenic diversity.) Therefore, if a virus—like HIV—can impair the immune system, then the same levels of antigenic diversity lead to a higher virus load. The maximum virus load is reached for lower levels of antigenic diversity (Fig. 4).

In our simulations, during the course of infection the average replication rate of the virus population increases. New antigenic variants are assigned random replication rates, but variants with higher replication rates have better chances of invading the existing population and also better chances of surviving subsequent invasions by other variants. Therefore, the average replication rate of the whole population will tend to increase during infection. Interestingly, we observe that in the model with

immune function impairment, the average replication rates increase faster than in the model without immune function impairment (Fig. 3).

In Section 5, we analysed a model where the immune response stimulation is described by the linear term, cy_i [see eqn (56)]. In this case, we observe that there is no limit to diversity. During infection, antigenic diversity can increase indefinitely albeit at a slower and slower rate. Simultaneously, virus load converges to its maximum level.

In earlier models without target cell limitation (Nowak *et al*., 1990; 1991), we found a critical level of antigenic diversity. If the antigenic diversity in a patient is below his or her characteristic threshold value then the virus population is controlled by immune responses, if the diversity exceeds this value then immune response control breaks down. Below the threshold there is a dynamic steady state between virus replication and CD4 cell levels, above the threshold there is uncontrolled virus growth. In models including target cell limitation, as described in this paper, we do not find the same separation of the dynamical behaviour of the system into two phases. Instead we find a maximum level of antigenic diversity and virus load. If antigenic diversity is at its maximum level then virus load is also at its maximum. Because of target cell limitation, the system always admits a steady state, even when the maximum diversity has been reached. But at this point, the virus population has completely escaped from control by specific immune responses.

Support from the Boehringer Ingelheim Fonds (R.R.R.) and the Wellcome Trust (D.W., M.A.N.) is gratefully acknowledged.

REFERENCES

Anderson, R. M. & May, R. M. (1989). In: *Cell to Cell Signaling* (Goldbeter, A., ed.), p. 335. New York: Academic Press.

Asjo, B., Albert, J., Karlsson, A., Morfeldtmanson, L., Biberfeld, G., Lidman, K. & Fenyo, E. M. (1986). Replication capacity of human immunodeficiency virus (HIV) from patients with varying severity of HIV infection. *Lancet* **2**(8508), 660–662.

Bittner, B., Bonhoeffer, S. & Nowak, M. A. (1997). Virus load and antigenic diversity. *Bull. Math. Biol.* (in press).

Bonhoeffer, S. & Nowak, M. A. (1997). Pre-existence and emergence of drug resistance in HIV-1 infection. *Proc. R. Soc.* **264,** 631–637.

Bonhoeffer, S., Holmes, E. C. & Nowak, M. A. (1995). Causes of HIV diversity. *Nature* **376**(6536), 125.

Bonhoeffer, S., Coffin, J. M. & Nowak, M. A. (1997a). Human immunodeficiency virus drug therapy and virus load. *J. Virol.* **71,** 3275–3278.

Bonhoerffer, S., May, R. M., Shaw, G. M. & Nowak, M. A. (1997b). Virus dynamics and drug therapy. *Proc. Natl. Acad. Sci. USA* **94,** 6971–6976.

Borrow, P., Lewicki, H., Wei, X. P., Horwitz, M. S., Peffer, N., Meyers, H., *et al*. (1997). Antiviral pressure exerted by HIV-1-specific cytotoxic T lymphocytes (CTLs) during primary infection demonstrated by rapid selection of CTL escape virus. *Nat. Med.* **3**(2), 205–211.

Cheynier, R., Henrichwark, S., Hadida, F., Pelletier, E., Oksenhendler, E., Autran, B. & Wainhobson, S. (1994). HIV and T cell expansion in splenic white pulps accompanied by infiltration of HIV-specific cytotoxic T lymphocytes. *Cell* **78**(3), 373–387.

DeBoer, R. J. & Boerlijst, M. C. (1994). Diversity and virulence thresholds in AIDS. *Proc. Natl. Acad. Sci. USA* **91,** 544–548.

DeBoer, R. J. & Boucher, C. A. B. (1996). Anti-CD4 therapy for AIDS suggested by mathematical models. *Proc. R. Soc. USA* **263,** 899–905.

Frost, S. D. W. & McLean, A. R. (1994). Quasispecies dynamics and the emergence of drug resistance during zidovudine therapy of HIV infection. *AIDS* **8,** 323–332.

Goulder, P. J. R., Phillips, R. E., Colbert, R. A., McAdam, S., Ogg, G., Nowak, M. A., *et al*. (1997). Late escape from an immunodominant cytotoxic T-lymphocute response associated with progression to AIDS. *Nat. Med.* **3**(2), 212–217.

Hahn, B. H., Shaw, G. M., Taylor, M. E., Redfield, R. R., Markham, P. D., Salahuddin, S. Z., Wong-Staal, F., Gallo, R. C., Parks, E. S. & Parks, W. P. (1996). Genetic variation in HTLV III/LAV over time in patients with AIDS or at risk for AIDS. *Science* **232,** 1548–1553.

Herz, A. V. M., Bonhoeffer, S., Anderson, R. M., May, R. M. & Nowak, M. A. (1996). Viral dynamics *in vivo*: limitations on estimates of intracellular delay and virus decay. *Proc. Natl. Acad. Sci. USA* **93,** 7247–7251.

Ho, D. D., Neumann, A. U., Perelson, A. S., Chen, W., Leonard, J. M. & Markowitz, M. (195). Rapid turnover of plasma virions and CD4 lymphocytes in HIV-1 infection. *Nature* **373,** 123–126.

Holmes, E. C., Zhang, L. Q., Simmonds, P., Ludlam, C. A., Leigh-Brown, A. J. (1992). Convergent and divergent sequence evolution in the surface envelope glycoprotein of HIV-1 within a single infected patient. *Proc. Natl. Acad. Sci. USA* **89,** 4835–4839.

Law, R. & Morton, R. D. (1993). Alternative permanent states of ecological communities. *Ecology* **74**(5), 1347–1361.

Lifson, J. D., Nowak, M. A., Goldstein, S., Rossio, J. L., Kinter, A., Vasquez, G., *et al*. (1997). The extent of early viral replication is a critical determinant of the natural history of simian immunodeficiency virus (SIV) infection. *J. Virol.* **71,** 9508–9514.

McLean, A. R. (1993). The balance of power between HIV and the immune system. *Trends in Microbiology* **1**(1), 9–13.

McLean, A. R. & Nowak, M. A. (1992a). Models of interactions between HIV and other pathogens. *J. theor. Biol.* **155,** 69–102.

McLean, A. R. & Nowak, M. A. (1992b). Competition between Zidovudine sensitive and Zidovudine-resistant strains in HIV. *AIDS* **6,** 71–79.

Meyerhans, A., Cheynier, R., Albert, J., Seth, M., Kwok, S., Sninsky, J., Morfeldt-Manson, L., *et al*. (1989). Temporal fluctuations in HIV quasispecies *in vivo* are not reflected by sequential HIV isolations. *Cell* **58,** 901–910.

Nee, S. & May, R. M. (1992). Dynamics of metapopulations: habitat destruction and competitive coexistence. *J. Animal Ecol.* **61**(1), 37–40.

Nowak, M. A. & Bangham, C. R. M. (1996). Population-dynamics of immune responses to persistent viruses. *Science* **272,** 74–79.

Nowak, M. A. & May, R. M. (1992). Coexistence and competition in HIV infection. *J. theor. Biol.* **159,** 329–342.

Nowak, M. A., May, R. M. & Anderson, R. M. (1990). The evolutionary dynamics of HIV-1 quasispecies and the development of immunodeficiency disease. *AIDS* **4,** 1095–1103.

Nowak, M. A., Anderson, R. M., McLean, A. R., Wolfs, T. F. W., Goudsmith, J. & May, R. (1991). Antigenic diversity thresholds and the development of AIDS. *Science* **254,** 963–969.

Nowak, M. A., May, R. M., Phillips, R. E., Rowland-Jones, S., Lalloo, D. G., McAdam, S., *et al*. (1995). Antigenic oscillations and shifting immunodominance in HIV-1 infections. *Nature* **375**(6532), 606–611.

Nowak, M. A., Anderson, R. M., Boerlijst, M. C., Bonhoeffer, S., May, R. M. & McMichael, A. J. (1996a). HIV-1 evolution and disease progression. *Science* **274,** 1008–1010.

Nowak, M. A., Bonhoeffer, S., Hill, A. M., Boehme, R., Thomas, H. C. & McDade, H. (1996b). Viral dynamics in Hepatitis B virus infection. *Proc. Natl. Acad. Sci. USA* **93**(9), 4398–4402.

Nowak, M. A., Bonhoeffer, S., Shaw, G. & May, R. (1997a). Antiviral drug treatment: dynamics of resistance in free virus and infected cell populations. *J. theor. Biol.* **184,** 205–219.

Nowak, M. A., Lloyd, A. L., Vasquez, G., Wiltrout, T. A., Bischofsberger, N., Williams, J., *et al*. (1997b). Viral dynamics of primary viremia and antiviral therapy in simian immunodeficiency virus infection. *J. Virol*., **71,** 7518–7525.

Perelson, a. S. (1989). Immune network theory. *Imm. Rev.* **110,** 5–36.

Perelson, A. S., Kirschner, D. E. & DeBoer, R. (1993). Dynamics of HIV-infection of CD4+ T-cells. *Math. Biosci.* **114,** 81–125.

Perelson, A. S., Neumann, A. U., Markowitz, M., Leonard, J. M. & Ho, D. D. (1996). HIV-1 dynamics *in vivo*: virion clearance rate, infected cell life-span and viral generation time. *Science* **271,** 1582–1586.

Perelson, A. S., Essunger, P., Cao, Y. Z., Vesanen, M., Hurley, A., Saksela, K., Markowitz, M. & Ho, D. D. (1997). Decay characteristics of HIV-1-infected compartments during combination therapy. *Nature* **387,** 188–191.

Phillips, R. E., Rowland-Jones, S., Nixon, D. F., Gotch, F. M., Edwards, G. P., Ogunlesi, A. O., *et al*. (1991). Human immunodeficiency virus genetic variation that can escape cytotoxic T cell recognition. *Nature* **354**(6353), 453–459.

Price, D. A., Goulder, P. J. R., Klenerman, P., Sewell, A. K., Easterbrook, P. J., Troop, M., *et al*. (1997). Positive selection of HIV-1 cytotoxic T lymphocyte escape variants during primary infection. *Proc. Natl. Acad. Sci. USA* **94**(5), 1890–1895.

Simmonds, P., Zhang, L. Q., McOmish, F., Balfe, P., Ludlam, C. A. & Brown, A. J. L. (1991). Discontinuous sequence change of human-immunodeficiency-virus (HIV) type 1 env sequences in plasma viral and lymphocyte associated proviral populations *in vivo*—implications for models of HIV pathogenesis. *J. Virol.* **65**(11), 6266–6276.

Stilianakis, N. I., Boucher, C. A. B., Dejong, M. D., Van-leeuwen, R., Schuurman, R. & DeBoer, R. J. (1997). clinical data sets of human-immunodeficiency-virus type-1 reverse-transcriptase-resistant mutants explained by a mathematical model. *J. Virol.* **71,** 161–168.

Tersmette, M., Gruters, R. A., DeWolf, F., DeGoede, R. E. Y., Lange, J. M. A., Schellekens, P. T. A., *et al*. (1989). Evidence for a role of virulent human immunodeficiency virus (HIV) variants in the pathogenesis of acquired immunodeficiency syndrome: studies on sequential HIV isolates. *J. Virol.* **63,** 2218–2125.

Wei, X., Gosh, S. K., Taylor, M. E., Johnson, V. A., Emini, E. A., Deutsch, P., *et al*. (1995). Viral dynamics in human immunodeficiency virus type 1 infection. *Nature* **373,** 117–122.

Wodarz, D., Klenerman, P. & Nowak, M. A. (1998). Dynamics of cytotoxic T lymphocyte exhaustion. *Proc. R. Soc. B* **265,** 191–203.

Wolinsky, S. M., Korber, B. T. M., Neumann, A. U., Daniels, M., Kunstman, K. J., Whetsell, A. J., *et al*. (1996). Adaptive evolution of human immunodeficiency virus type 1 during the natural course of infection. *Science* **272**(5261), 537–542.